Metabolomics (2026) 22:32
https://doi.org/10.1007/s11306-026-02414-8

ORIGINAL ARTICLE

Exploring metabolic signatures in urine using NMR for improved prognosis of gliomas

Aditi Pandey[1,2] · Aanchal Datta[3] · Rajeev Verma[1] · Awadhesh Kumar Jaiswal[3] · Raj Kumar[3] · Kuntal Kanti Das[3] · Bikash Baishya[1,2]

Received: 19 June 2025 / Accepted: 17 February 2026 / Published online: 6 March 2026
© The Author(s) 2026

Abstract

Introduction Gliomas represent the tumors of the central nervous system that originate from glial cells. Overall survival predictions and treatment regimen selection are based on accurate tumor diagnosis and grading. However, the diagnosis of glioma remains critically dependent on either invasive biopsies or advanced imaging.

Objective This exploratory study aims to assess the diagnostic potential of urine specimens for discriminating gliomas from controls and identify the dysregulated pathways in a North Indian cohort. Urine is an ideal non-invasive candidate, requires no prior preparation, and considerably increases patient compliance.

Method Urine samples from 50 glioma patients were analysed with ^{1}H NMR (Nuclear Magnetic Resonance) spectroscopy and compared with those of healthy controls. Statistical analysis was performed in MetaboAnalyst 6.0 to identify significantly perturbed metabolites. Diagnostic performance was assessed using the Receiver Operating Characteristic (ROC) curve, and the Random Forest model was used to evaluate classification accuracy. Pathway enrichment and topology analysis based on the KEGG (Kyoto Encyclopedia of Genes and Genomes) database were performed to identify dysregulated pathways.

Results ^{1}H NMR metabolic analysis of urine samples revealed seven statistically significant ($p<0.05$) metabolites namely acetate, pyruvate, creatinine, dimethylamine, glutamine, alanine and carnitine. This panel of metabolites displayed excellent diagnostic capability with an Area Under the Curve of 0.90 as measured by a multivariate ROC curve. The random forest model efficiently differentiated glioma from control samples using significant metabolites. Disruption in the primary energy pathways of the body and in the metabolism of major amino acids was observed in the pathway analysis.

Conclusion Integration of these urinary signatures into current clinical practice can serve as an additional diagnostic tool and a non-invasive screening method for populations at risk. They can also be monitored in real time, thus aiding in adaptive treatment strategies and therapy assessment.

Keywords Glioma · Metabolomics · Nuclear magnetic resonance (NMR) · Metaboanalyst · Cancer

Abbreviations

AUC	Area under the curve
BMRB	Biological magnetic resonance bank
CNS	Central nervous system
HMDB	Human metabolome database
HSQC	Heteronuclear single quantum coherence
KEGG	Kyoto encyclopedia of genes and genomes
NMR	Nuclear magnetic resonance
NOESY	Nuclear overhauser effect spectroscopy
PCA	Principal component analysis
PDH	Pyruvate dehydrogenase
PDK	Pyruvate dehydrogenase kinase
PLS-DA	Partial least square discriminant analysis
ROC	Receiver operator characteristic

✉ Bikash Baishya
bikashbaishya@gmail.com

Kuntal Kanti Das
kkdas@sgpgi.ac.in

[1] Centre of Biomedical Research, Lucknow, Uttar Pradesh, India

[2] Academy of Scientific and Innovative Research (AcSIR), Ghaziabad 201002, India

[3] Department of Neurosurgery, Sanjay Gandhi Postgraduate Institute of Medical Sciences, Lucknow, Uttar Pradesh, India

TOCSY Total correlation spectroscopy
WHO World health organisation

1 Introduction

Gliomas are a type of central nervous system (CNS) tumor that arise in glial cells and then invade the brain parenchyma. They are predominant and most aggressive primary brain tumors, accounting for about 80% of all brain malignancies (Hanif et al., 2017). Gliomas encircle astrocytic tumors (astrocytoma, anaplastic astrocytoma and glioblastoma), oligodendrogliomas, ependymomas, and mixed gliomas, among which glioblastoma is the most malignant and frequently occurring (Ohka et al., 2012). Glioma was classified based on histological features, but due to several limitations, the WHO (World Health Organisation) revised this classification in 2021 to include molecular pathology and a genetic perspective as well (Louis et al., 2021).

In the case of glioblastomas, despite being identified for the first time in 1863 by Rudolf Virchow, there is still no effective targeted therapy (Virchow, 1863–1867). Currently, MRI is predominantly used for diagnosis and monitoring of gliomas; however, it often lacks specificity in distinguishing metastases from primary tumors and pseudoprogression from true progression (Neska-Matuszewska et al., 2018). Therapeutic strategies involve maximal safe surgical resection followed by radiotherapy and chemotherapy. Nevertheless, the vast majority of glioma cases experience tumor recurrence after initial treatment and limited responsiveness to subsequent lines of therapy (Shergalis et al., 2018). Standard prescribed drugs, including temozolomide, confer only modest benefits and are frequently associated with adverse effects (Chamberlain, 2010).

Evidently, the inter and intratumoral heterogeneity of gliomas makes them challenging to treat and contributes to therapy resistance and recurrence (Sottoriva et al., 2013). There is a need for reliable and non-invasive biomarkers that overcome the limitations associated with imaging, tumor heterogeneity, and the blood-brain barrier.

At first, glioma manifests itself with common symptoms like headache, nausea, blurred vision, etc., which are easily ignored, and the tumor advances even before the person gets to know. These symptoms result from increased intracranial pressure, edema and infiltration of functional brain regions (Weller et al., 2015). Metabolic programming is greatly rewired by glioma to sustain its growth, and these changes in the metabolite pattern can occur years before clinical presentation (Björkblom et al., 2016; Jonsson et al., 2020). Due to the direct impression of metabolic activity that it provides, metabolomics has been extensively used for biomarker studies in malignancies of prostate, breast, kidney and colon, among others (Brezmes et al., 2022; Budczies et al., 2012; Cheng et al., 2019; DeFeo et al., 2011; Gao et al., 2012).

Metabolomics characterizes the small-molecule downstream products of genomic and proteomic processes in the body and thus provides a direct representation of the biochemical phenotype (Horgan & Kenny, 2011). Among the analytical techniques employed for metabolomics, NMR has been playing a pivotal role due to its robustness, high degree of reproducibility, easy sample preparation, quantitative and non-destructive nature (Markley et al., 2017). It enables simultaneous detection and quantification of a broad range of metabolites, making it valuable for biomarker research. NMR spectroscopy has been extensively used in glioma metabolomics for tissue and biofluid analysis (Jothi et al., 2020; Kelimu et al., 2016; Lee et al., 2019).

For a considerable time, urine has served as a valuable biofluid in human health assessment, as reflected by early observations such as the link between sweet-tasting urine and diabetes mellitus or the presence of albumin in urine as a marker of kidney disease (Armstrong, 2007). Advancement of omics technologies has enabled comprehensive analysis of liquid biopsies (Dinges et al., 2019) facilitating insights into the disease biology, biomarker discovery, progression and monitoring as well as therapy response (Amelio et al., 2020; Diaz et al., 2023; Mukherjee et al., 2024).

Urine NMR metabolomics has been a well-established tool in disease research, whether it be for epidemiology studies, differential diagnosis, early screening or tracking prognosis and treatment (Bruzzone et al., 2020; Chasapi et al., 2022; Tynkkynen et al., 2019; Yu et al., 2025). Using urine for NMR-based metabolomics is advantageous as it allows for non-invasive collection and direct spectral acquisition without prior processing or extraction, thus permitting large-scale screening (Bouatra et al., 2013; Ruiz-Rodado et al., 2021). Larkin et al., 2016 demonstrated that brain metastases can be diagnosed from micrometastatic stages using urinary metabolomics, highlighting the clinical translational potential of this approach. Few studies have analysed the metabolic profile in urine to understand gliomas through mass spectroscopy (Shi et al., 2021; Tandle et al., 2013), but urinary NMR metabolomics remains relatively unexplored in glioma research.

Using NMR-based metabolomics and urine as the sample, we aim to detect and simultaneously quantify metabolites that can distinguish glioma cases from controls in the North Indian cohort, as region specific dietary habits, environment and genetic background influence the metabolome. We have compared control vs. individual grades as well as control vs. combined grades.

Candidate biomarkers can assist in diagnosis, and corresponding altered pathways can help provide a deeper

understanding of the disease's pathogenesis and monitor response to treatment.

2 Materials and method

This study included patients with diffuse gliomas (WHO grades 2, 3, and 4; astrocytoma, oligodendroglioma, and oligoastrocytoma not otherwise specified), histologically classified according to the fifth edition of the WHO classification. Adults aged 16 years or older were included, and these patients underwent stereotactic biopsy and resective surgery at the Department of Neurosurgery, Sanjay Gandhi Post Graduate Institute of Medical Sciences (SGPGIMS), Lucknow, during October 2020 to March 2022. All the subjects provided well-informed written consent.

2.1 Sample collection

First pass morning urine collected midstream in sterile urine containers immediately pre-operative, was taken from the patients to which sodium azide was added and then it was stored at −80° C until analysis.

Table 1 Clinical characteristics of the glioma cases included in the study showing age, gender, type and duration of the symptoms shown by the patients

Characteristics	N (%)
Age	
Study – Mean ($n=50$)	42.3 years
Control – Mean ($n=10$)	44.8 years
Gender	
Study ($n=50$)	
Male	33 (66)
Female	17 (34)
Control ($n=10$)	
Male	2 (20)
Female	8 (80)
KPS on admission	
<80	20 (40)
≥80	30 (60)
KPS on discharge	
<60	10 (20)
≥60	40 (80)
Duration of symptoms	
Mean	19.74 months
Median (IQR)	5.5 months (15.25)
Headache	28 (56)
Vomiting	3 (6)
Seizures	29 (58)
Motor deficit	14 (28)
Sensory deficit	2 (4)
Cranial nerve deficit	9 (18)

2.1.1 Inclusion criteria

1. >16 years and <65 years of age.
2. Histologically confirmed astrocytoma or oligodendroglioma or their combination.
3. Operated for the first time at SGPGI.

2.1.2 Exclusion criteria

1. Lack of consent.
2. Children<16 years.
3. Recurrent gliomas.
4. Any other comorbidities such as chronic kidney disease, diabetes, significant liver dysfunction and other active infection.

The patients were evaluated according to the department's protocol, taking into account their clinical history and standard neurological examination. Contrast-enhanced MRI was performed for all patients. Based on the tumor's size, location, and symptoms, either stereotactic biopsy or open surgery was performed. Following this, adjuvant therapy was given and histopathological diagnosis was documented.

Table 1 summarises the clinical characteristics of the gliomas, while Table 2 shows the radiological characteristics of the tumors. Histopathologically, 44% (22 cases) of the tumors were Grade 2, followed by Grade 4 (34%, 17 cases), and the remaining 22% (11 cases) were Grade 3. All the grade 4 tumors were of IDH wild type. Histopathological characters are listed in Table 3.

In the patient group comprising 50 individuals, 33 patients were male, and 17 were female (M: F≈2:1). The mean age of the patients was 42.3 years (range 18–84 years). BMI data was available for a subset of patients and these values were in the normal BMI range according to Indian reference standard. The symptoms persisted for a mean of 19.7 months. Headache and seizures were the most frequently observed symptoms. 28% ($n=8$) of the cases had some form of motor deficit.

Ten healthy individuals (8 female, 2 male) with an average age of 44.8 years, no history of neurological disorder or systemic disease and no prescribed medication were taken as the control group for the study. Sample collection and storage methods were identical between the groups.

2.2 Sample preparation for NMR spectroscopy

The urine samples were thawed at room temperature, then vortexed and centrifuged (at 10,000 rpm for 5 min at 4 °C) to remove unwanted particulates. 540 µL of urine from the

Table 2 Radiological features of the tumor highlighting the location, size, lobes involved and whether or not characteristics like cystic degeneration, enhancement and calcification are present

Characteristics	N (%)
Side of tumor	
Left	20 (40)
Right	27 (54)
Bilateral	3 (6)
Size	
<4 cm	13 (26)
≥4 cm	37 (74)
Preoperative hydrocephalus	1 (2)
Location of tumors	
Frontal	21 (42)
Temporal	16 (32)
Insula	4 (8)
Parietal	4 (8)
Corpus callosum	3 (6)
Occipital	1 (2)
Thalamus	1 (2)
Lobes involved	
1	30 (60)
2	18 (36)
3	2 (4)
Cystic degeneration	14 (28)
Enhancement	31 (62)
Calcification	1 (2)
Hemisphere	
Confined to one	45 (90)
Involving both	5 (10)

Table 3 Histopathological characteristics of the tumor showing the grades and type

Characteristics	N (%)
Glioma type	
Glioblastoma	17
Other types	33
WHO grade	
Gr II	22 (44)
Gr III	11 (22)
Gr IV	17 (34)

top layer was mixed with 60 µL of Phosphate Buffer in D_2O containing 0.5 mM TSP in an Eppendorf tube. After vortexing the mixture, 550 µl was transferred to a 5-mm NMR tube (Wilmad, USA).

2.3 NMR measurements

Experiments were performed on BRUKER AVANCE III 800-MHz NMR spectrometer equipped with CPTCI cryoprobe. 1D NOESY spectra with water presaturation (Araníbar et al., 2006) using the sequence noesypr1d (as per Bruker's pulse program library) were recorded for each sample. The spectra thus obtained were pre-processed using TopSpin v3.6.1, including phase correction and baseline adjustment. The acquisition parameters were as follows: spectral width of 20 ppm with 192 scans (8 dummy scans), 64 k data points, an acquisition time of 3s, and a relaxation delay of 6.5s. Calibration was done by taking the TSP resonance at δ (0) as a reference. 2D spectra comprising HSQC (Heteronuclear Single Quantum Coherence), TOCSY (Total Correlation Spectroscopy), and J-RES (J-resolved) spectra were recorded for the pooled sample.

2.4 Metabolite assignment

1D-^{1}H NMR spectra of the urine samples outline the array of metabolites represented by the different peaks. Resonances were assigned using chemical shift libraries available in databases such as HMDB (Human Metabolome Database, https://www.hmdb.ca/) and BMRB (Biological Magnetic Resonance Bank, https://bmrb.io/). For further verification of the assignment, 2D spectra including TOCSY, HSQC, and *J*-RES were used. Chemical shift values of the assigned metabolites are listed in Table 4. Quantification was performed using TSP as the reference, with curve fitting in Chenomx NMR Suite v8.4 (Chenomx Inc., Edmonton, AB, Canada).

2.5 Data filtering

Samples were excluded if the recorded spectra were of low quality (very low signal to noise ratio, prominent artefact peaks obscuring the metabolites of interest, distorted baselines). Samples lying outside the 95% confidence ellipse in the initial PCA of the normalized spectra were considered as outliers and were also excluded. In this way, a total of 15 samples (10 from grade 2, 2 from grade 3 and 3 from grade 4) were filtered from the study.

2.6 Statistical analysis

Multivariate data analysis was performed using Metaboanalyst 6.0 https://www.metaboanalyst.ca/ (Pang et al., 2024). The data was normalized by sum to correct for dilution differences, log-transformed to minimize skewness and auto-scaling was done before multivariate analysis. The metabolite patterns were compared between control vs. diseased (all grades combined), control vs. grades 2, 3 and 4 and control vs. individual grades. Unsupervised Principal Component Analysis (PCA) was initially performed to identify trends and outliers in the data, followed by supervised Partial Least Squares Discriminant Analysis (PLS-DA) with 5-fold cross-validation to assess group clustering and differences. Variable Importance in Projection (VIP) scores were evaluated using PLS-DA. Permutation analysis was performed to determine whether the results were significant. *t*-test and ANOVA (Analysis of Variance) were used

Table 4 Table showing the assigned metabolites confirmed through Chenomx and 2D spectra. Chemical shifts of proton and carbon are depicted

S.N.	Metabolite	^{1}H Shift (ppm)	^{13}C (ppm)	J-coupling (Hz)	Methods used
1.	2-hydroxybutyrate	0.87(t)	11.80	7.41	1-D, Chenomx, J-*RES*
		1.73(m)	–	–	
		4(dd)	–	–	
2.	2-hydroxyisobutyrate	1.36(s)	29.60	–	1-D, Chenomx, HSQC
3.	3-aminoisobutyrate	1.18(d)	17.80	–	1-D, Chenomx, J-*RES*, TOCSY
		2.60(m)	42.10	–	
		3.02(dd)	45.10	–	
		3.09(dd)	45.10	–	
4.	3-Hydroxyisovalerate	1.27(s)	30.87	–	1-D, Chenomx, HSQC
		2.37(s)	52.33	–	
5.	Acetate	1.92(s)	26.08	–	1-D, Chenomx, HSQC
6.	Adenine	8.17(s)	–	–	1-D, Chenomx
		8.19(s)	–	–	
7.	Alanine	1.48(d)	19.07	–	1-D, Chenomx, HSQC, TOCSY
		3.78(q)	53.30	–	
8.	Allantoin	5.38(s)	66.05	–	1-D, Chenomx, HSQC
9.	Betaine	3.25(s)	56.01	–	1-D, Chenomx, HSQC
		3.89(s)	–	–	
10.	Carnitine	2.44(m)	45.70	–	1-D, Chenomx, HSQC, TOCSY
		3.23(s)	56.99	–	
		3.42(m)	72.68	–	
11.	Citrate	2.55(d)	47.33	–	1-D, Chenomx HSQC, TOCSY
		2.70(d)	47.80	–	
12.	Creatine	3.03(s)	39.88	–	1-D, Chenomx, HSQC
		3.93(s)	56.81	–	
13.	Creatinine	3.04(s)	33.08	–	1-D, Chenomx, HSQC
		4.05(s)	59.29	–	
14.	Dimethyl sulfone	3.14(s)	44.12	–	1-D, Chenomx, HSQC
15.	Dimethylamine	2.73(s)	37.44	–	1-D, Chenomx, HSQC
16.	Formate	8.44(s)	174	–	1-D, Chenomx
17.	Gluconate	3.65(m)	65.39	–	1-D, Chenomx HSQC, TOCSY
		3.75(m)	75.40	–	
		3.82(m)	65.39	–	
		4.02(m)	73.65	–	
		4.12(d)	76.74	–	
18.	Glutamine	2.15(m)	29.20	–	1-D, Chenomx, HSQC, J-*RES*, TOCSY
		2.44(m)	33.92	–	
		3.77(t)	57.20	6.16	
19.	Glycine	3.57(s)	44.67	–	1-D, Chenomx, HSQC
20.	Glycolate	3.95(s)	64.05	–	1-D, Chenomx, HSQC
21.	Hippurate	3.97(d)	46.75	–	1-D, Chenomx HSQC, TOCSY
		7.55	131.75	–	
		7.63(tt)	135.25	–	
		7.83(dd)	130.06	–	
22.	Histidine	3.16(dd)	27.60	–	1-D, Chenomx HSQC, TOCSY
		3.23(dd)	27.60	–	
		3.98(dd)	56.10	–	
		7.09(s)	127.00	–	
		7.90(s)	141.10	–	
23.	Isobutyrate	1.06(d)	–	7.02	1-D, Chenomx, J-RES
		2.36(m)	–	–	
24.	Lactate	1.33(d)	22.80	–	1-D, Chenomx HSQC, TOCSY
		4.12(q)	71.69	–	
25.	N, N-Dimethylglycine	2.93(s)	46.40	–	1-D, Chenomx, HSQC
		3.72(s)	61.62	–	
26.	Propylene glycol	1.14(d)	20.89	6.44	1-D, Chenomx HSQC, TOCSY, J-RES
		3.44(dd)	69.41	–	
		3.54(dd)	69.43	–	
		3.88(m)	70.85	–	

Table 4 (continued)

S.N.	Metabolite	^{1}H Shift (ppm)	^{13}C (ppm)	J-coupling (Hz)	Methods used
27.	Pyruvate	2.38(s)	29.40	–	1-D, Chenomx, HSQC
28.	Succinate	2.42(s)	37.10	–	1-D, Chenomx, HSQC
29.	Trigonelline	4.44(s)	51.20	–	1-D, Chenomx HSQC, TOCSY, J-RES
		8.71(m)	149.33	–	
		8.97(m)	147.29	–	
		9.10(m)	147.29	–	
30.	Trimethylamine	4.88(s)	45.49	–	1-D, Chenomx, HSQC
31.	Trimethylamine N-oxide	3.25(s)	62.19	–	1-D, Chenomx, HSQC

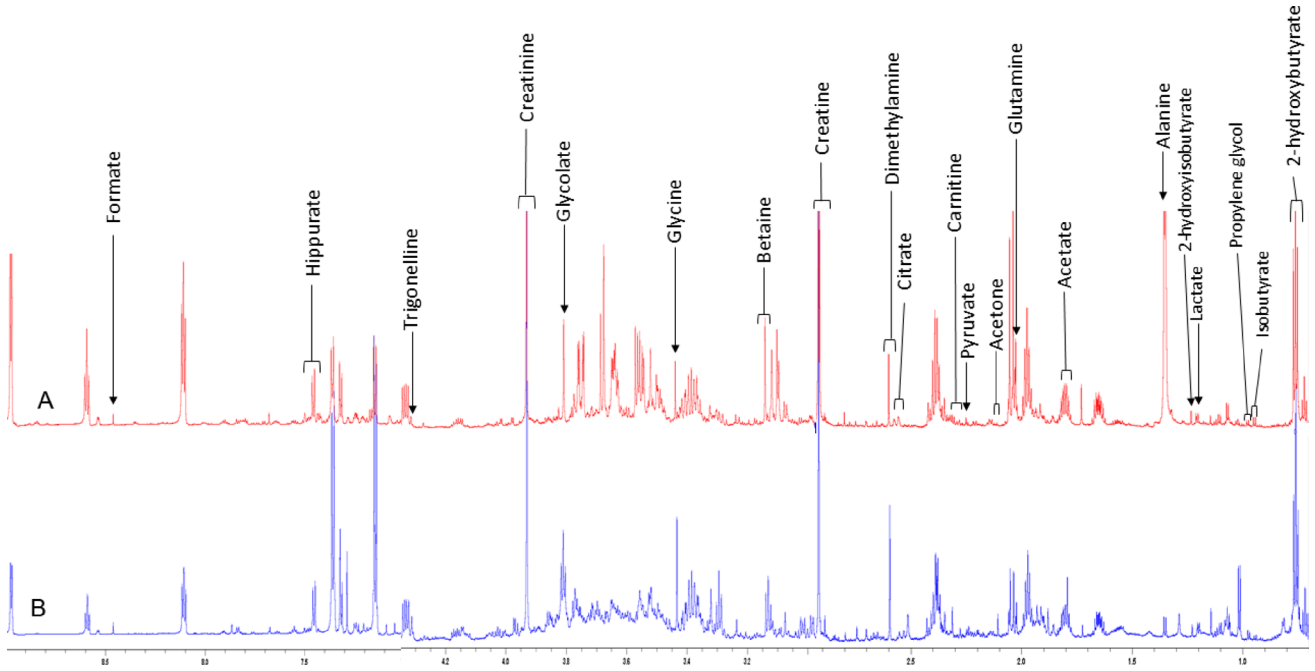

Fig. 1 A representative 1D NOESY spectra of urine sample from patients (**A**) and control (**B**) highlighting some of the prominent metabolite peaks

to identify significant metabolites in two- and multiple-group comparisons, respectively. Bonferroni correction was applied to reduce the false discovery rate. Cohen's d effect size was calculated for the significant features in control vs. disease comparison to account for the limited sample size. Random forest was used as a complementary tool to assess variable importance, followed by constructing mean decrease in accuracy (MDA) plot that show the model's accuracy loss as each metabolite is removed.

Pathway analysis, that integrates enrichment and topology scoring, based on KEGG database, was performed to reveal the pathways that were most disrupted.

Receiver Operating Characteristic (ROC) curve analysis was performed to assess how well the model predicts the classes. Significant metabolites found through the *t*-test were used to construct the curve.

3 Result

3.1 ^{1}H NMR spectroscopy

A total of 35 spectra of glioma samples were included in the analysis, comprising 12 from grade 2, 9 from grade 3 and 14 from grade 4. Figure 1 depicts a representative 1D NOESY spectrum from the urine samples of diseased (1A) and control (1B) individuals, showing some of the prominent peaks, while detailed assignment with respective chemical shifts is listed in Table 4. 31 metabolites were identified, including amino acids such as alanine, glutamine, histidine, pyruvate; organic acids like pyruvate, lactate, acetate; energy compounds like glucose, creatinine and creatine among others.

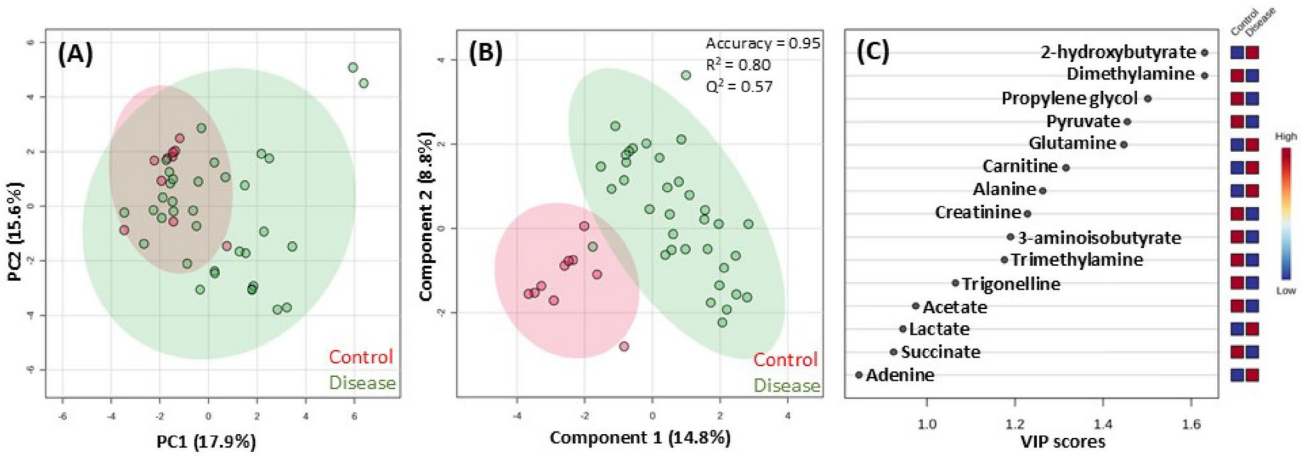

Fig. 2 Multivariate statistical analysis done on Control vs. Disease group using Metaboanalyst 6.0 on the urine samples. **A** Unsupervised Principal Component Analysis (PCA) Score Plot for Control vs. Glioma depicting significant clustering between the two groups. **B** Supervised Partial Least Square Discriminant Analysis (PLS-DA) Score Plot for Control vs. Glioma shows the separation between groups while taking into account the class labels. **C** VIP Score Plot for Control vs. Glioma, metabolites having Variable Importance in Projection (VIP) Score of >1 are considered important for separation between the two classes

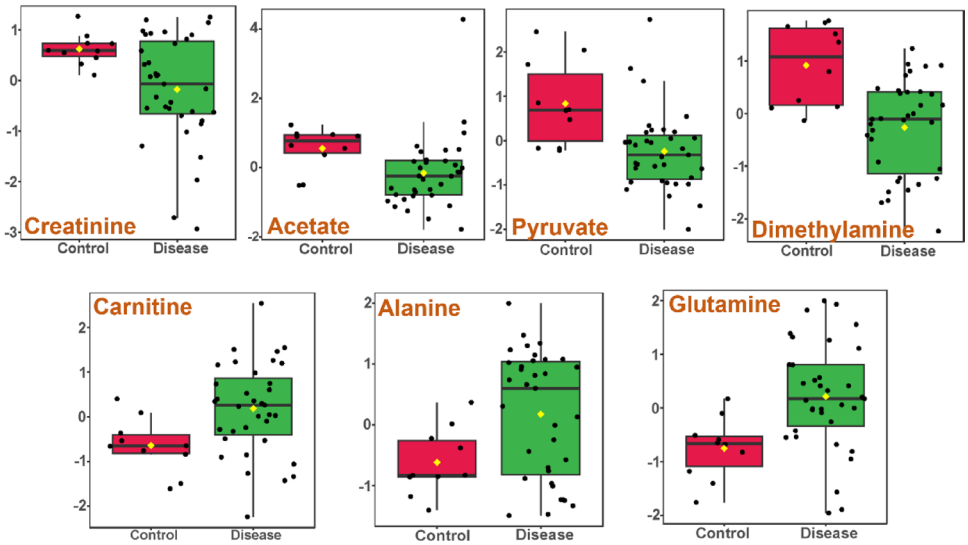

Fig. 3 Box plot of metabolites that were significantly altered between Control and Disease groups as obtained through *t*-test, glutamine, alanine and carnitine were found to be upregulated in disease condition whereas acetate, pyruvate, creatinine and dimethylamine were downregulated

3.2 Multivariate analysis and metabolic fingerprinting

3.2.1 Glioma vs. control

PCA score plot shows cluster formation but the features overlap for some of the samples (Fig. 2A). PLS-DA done taking into account the class labels, showed clear group separation (Fig. 2B). The model displayed significantly good fit and predictive power as the parameters associated with the model i.e. R^2 which indicates the goodness of fit and Q^2, that shows the predictive capability of the model were high ($R^2 = 0.80$, $Q^2 = 0.57$). Random permutation test ($n = 1000$) yielded a p-value of 0.001, further proving that the difference is not due to chance.

The metabolites with maximum VIP score were 2-hydroxybutyrate, dimethylamine, propylene glycol, pyruvate, glutamine, carnitine, alanine, creatinine, 3-aminoisobutyrate, trimethylamine and trigonelline (Fig. 2C). Seven metabolites were found to be significant out of which acetate, pyruvate, creatinine and dimethylamine were downregulated and glutamine, alanine and carnitine were upregulated (Fig. 3). All the significant features had large effect sizes ($d > 0.8$), except for acetate, which still had moderate effect size (0.73), as listed in Table S1 of SI.

Random forest classification using 1000 decision trees for the control vs. diseased group showed an out-of-the-box (OOB) error of 8.9% (Fig. 4A). This error was due to class imbalance arising from the small sample size of controls. Consistent results were seen in MDA plot (Fig. 4B), where 2-hydroxybutyrate, dimethylamine, pyruvate, acetate,

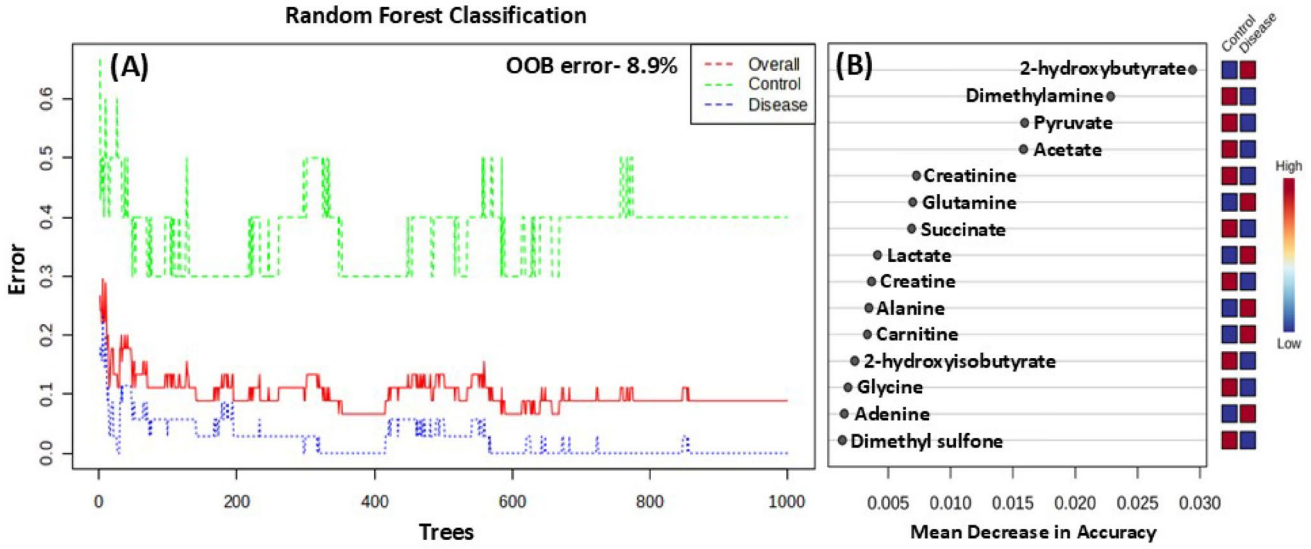

Fig. 4 **A** The out of the box (OOB) error came out to be 8.9% wherein the model correctly classified all the disease samples. **B** Random Forest uses mean decrease in accuracy as a measure to identify feature's importance, which overlooks the decrease in prediction accuracy as the values of the specific feature is permuted in out of bag observations

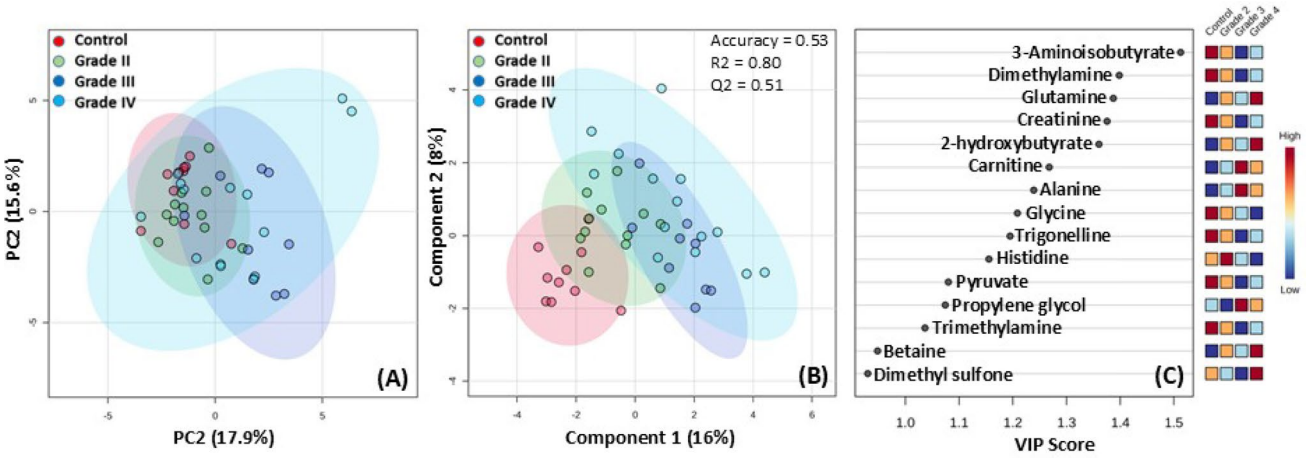

Fig. 5 Multivariate Statistical Analysis taking into account Control vs. Different grades of Glioma together. **A** PCA Score Plot for Control vs. Different Glioma grades, clustering is not very distinct and some data points from different groups tend to overlap. **B** PLS-DA Score Plot for Control vs. Different Glioma grades showing the gradual shift of the different clusters as the severity of grades increases. **C** VIP Score Plot displaying top metabolites that are bringing about the separation

creatinine and glutamine were the top features leading to reduction in classification accuracy when permuted.

3.3 Different glioma grades vs. control

Although the clusters are seen as somewhat merged in the dimensionality reduction analysis (Fig. 5A, B), the groups gradually tend to separate from each other. This separation is higher in PLS-DA. More severe glioma grades were more distinct from the control, whereas low-grade gliomas were relatively close to it. PLS-DA was cross-validated to ensure there was no overfitting ($R^2 = 0.80$, $Q^2 = 0.51$). To further ensure the model's predictability, a permutation test was performed, yielding a p-value of 0.01. 3-aminoisobutyrate, dimethylamine, glutamine, creatinine, 2-hydroxybutyrate, carnitine, alanine, glycine, trigonelline, histidine, pyruvate, propylene glycol and trimethylamine had maximum VIP scores (Fig. 5C). Analysis of Variance (ANOVA) showed 2-hydroxybutyrate, pyruvate, creatinine, dimethylamine and dimethyl sulfone to be significant; group comparisons having p value < 0.05 were annotated with '*' (Fig. 6). Mean SD plot for all the metabolites is given in Fig S1 of SI, where some metabolites show progressive change from control to higher grades, and some showing more variability in higher glioma grades, highlighting the metabolic heterogeneity of glioma.

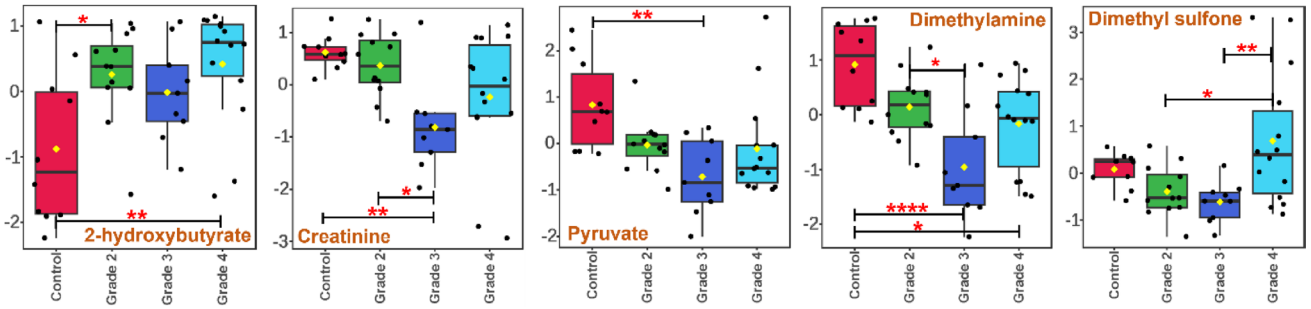

Fig. 6 Box plot of the metabolites identified to be significantly perturbed through ANOVA in comparison of Control with the different grades. 2-hydroxybutyrate was upregulated while pyruvate, creatinine and dimethylamine were downregulated in all the grades when compared with control. Group comparisons with significant p-value are marked with star (*). Number of star i.e. '*', '**', '***' and '****' correspond to p-values less than 0.05, 0.01, 0.001 and 0.0001 respectively

Multivariate analysis was performed to compare the glioma grades individually with the control cases. It is clear from Fig. 7 that, across all three grades, a clear difference was observed as they clustered separately from healthy controls.

Pathway analysis revealed major perturbation in the following pathways- (1) Glycine, Serine and Threonine metabolism, (2) Pyruvate metabolism, (3) Histidine metabolism, (4) Glyoxylate and dicarboxylate metabolism, (5) Citrate (TCA) cycle, (6) Glycolysis/Gluconeogenesis, (7) Alanine, aspartate and glutamate metabolism (Fig. 8). A graphical representation is shown in Fig. 9.

Area under the curve in multivariate ROC analysis (Fig. 10) for the significant metabolites was 0.90 for Control vs. Diseased (95% CI 0.76 to 0.98), indicating that the model distinguished the groups with high sensitivity and specificity and had excellent diagnostic potential.

Table 5 reveals the discriminatory metabolites identified as important in the fold change analysis and with VIP values > 0.90. The variance explained by the principal components in PCA, the R^2 and Q^2 from PLS-DA cross-validation, and the p-values obtained from permutation test across 1000 iterations in the different cases are shown in Table 6.

4 Discussion

Glioma manifests itself as a highly aggressive and fatal brain tumor, having an array of complications and heterogeneity with limited treatment options; therefore, patients with glioma need to be treated with utmost care and minimally invasive tests and monitoring methods must be devised to look over the condition.

Metabolomics has proven to be an efficient technique for novel biomarker discovery and understanding underlying biochemical pathways. Urine metabolomics is beneficial as it requires no prior preparation, is non-invasive and increases patient compliance considerably. Moreover, in conditions such as glioma, where there are several critical health risks, urine-based tests will be highly advantageous. Although the urine composition may vary due to factors such as age, diet, hydration status, etc., we have minimized these variations by following the same procedure of urine collection for all the subjects and scaling, log transformation and normalization of the concentration profile (Emwas et al., 2016).

Creatinine has a major role in energy metabolism. There is a significant decrease in levels of muscle-derived metabolites in biofluids in the case of sarcopenia i.e., muscle wasting (Stretch et al., 2012) and often secondary sarcopenia is seen in patients suffering from cancer, wherein cancer cachexia and metabolic dysregulation can cause muscle atrophy, thus reducing creatinine production and excretion. Increased consumption of creatine phosphate by aggressive tumors to meet their energy requirement may also lead to lower levels of its breakdown product, i.e. creatinine (Wyss & Kaddurah-Daouk, 2000), which is also in accordance with previous reports that suggest creatinine levels tend to be lower in high-grade tumors (Baranovičová et al., 2019; Mörén et al., 2015).

Urinary excretion of 2-hydroxybutyric acid can be a readout of systemic oxidative stress as it is produced from 2-oxobutyrate that arises as a result of increased glutathione flux through the trans-sulfuration pathway (Ponti et al., 2024). It was correlated with cases of lactic acidosis or ketoacidosis, which is common in cancer patients, as the energy balance is highly disturbed (Zhao et al., 2024).

Dimethylamine is formed by degradation of symmetric and asymmetric dimethylarginine, post-translational methylation of arginine residues catalysed by protein arginine methyltransferases and through microbial metabolism of methylamine (Tain & Hsu, 2017; Tang et al., 2013). To compensate for the heightened requirement of methyl groups associated with the DNA and histone modifications and epigenetic changes (particularly hypermethylation), methylamines may be increasingly diverted to one carbon

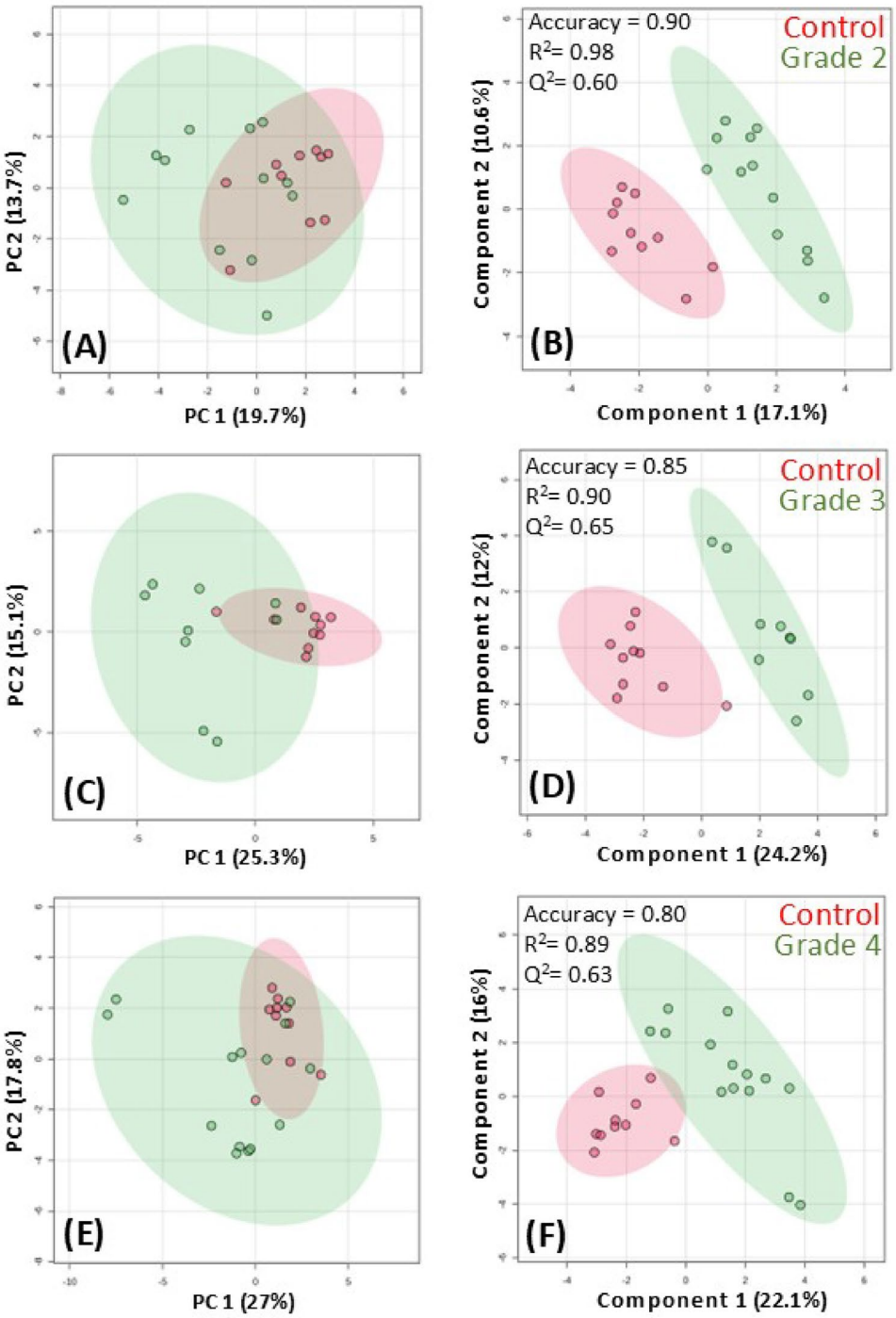

Fig. 7 **A** PCA Score plot of control vs. grade 2, **B** PLS-DA Score plot of control vs. grade 2, **C** PCA Score plot of control vs. grade 3, **D** PLS-DA Score plot of control vs. Grade 3, **E** PCA Score plot of control vs. grade 4, **F** PLS-DA Score plot of control vs. grade 4.Clustering improves to some extent in PCA Score plots as the severity of grades progresses. Clear discrimination is seen in PLS-DA Score plot in all the cases, values of accuracy, R^2 and Q^2 from cross-validation of the models is mentioned

metabolism (Locasale, 2013), thus decreasing their renal excretion. Moreover, glioma patients exhibit gut dysbiosis with depletion of microflora involved in methylamine metabolism (Wang et al., 2024), further leading to reduced urinary dimethylamine levels.

Glioma cells also exploit fatty acids for harnessing energy and NADH, NADPH, and FADH2 are needed for cellular growth and proliferation (Carracedo et al., 2013). It was assumed that glioma cells rely on aerobic glycolysis predominantly; however, Maher et al., 2012 studied the metabolism of human brain tumor in situ and concluded that less than half of the Acetyl-CoA pool was derived from glucose, which means that apart from the Warburg effect, there is significant fatty acid oxidation (FAO) in glioma cells (Lin et al., 2016). For FAO, carnitine is crucial. Despite being recycled, carnitine also plays a role in other cellular processes; hence, cells require sustained carnitine availability. Elevated urinary carnitine levels may be a byproduct of

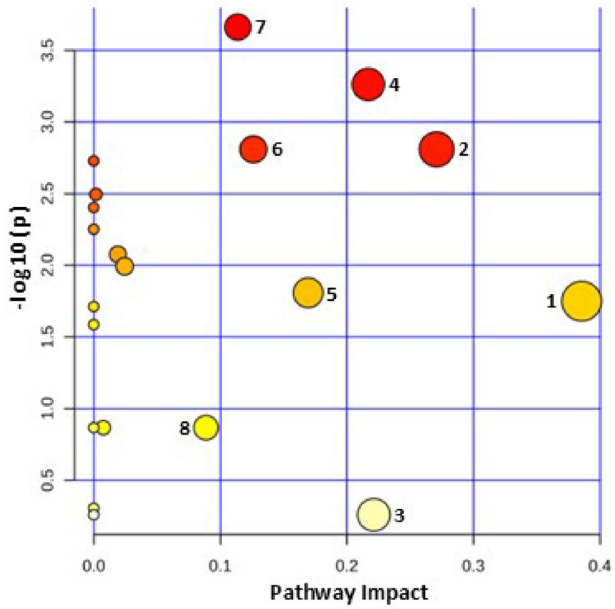

Fig. 8 Pathway analysis module of Metaboanalyst 6.0 incorporates p values from enrichment analysis and pathway impact values from topology analysis to highlight the disturbed pathways. Pathways having impact > 0.08 were considerably perturbed which include 1. Glycine, serine and threonine metabolism, 2. Pyruvate metabolism, 3. Histidine metabolism, 4. Glyoxylate and dicarboxylate metabolism, 5. Citrate (TCA) cycle, 6. Glycolysis/Gluconeogenesis, 7. Alanine, aspartate and glutamate metabolism and 8. Glutathione metabolism

the tumor's increased demand for FAO, increasing carnitine turnover and total flux. Solute carriers (SLC) coding genes SLC6 and members of SLC22 are responsible for the movement of hydrophilic carnitine inside the cell (Juraszek et al., 2021), among which SLC22A5 (Fink et al., 2019) is a high-affinity transporter of carnitine and is found to be overexpressed in primary and recurrent glioblastomas; other carnitine transporters that regulate its homeostasis are dysregulated in cancers (Console et al., 2020). Additionally, gut dysbiosis evident in glioma can also lead to altered carnitine metabolism and excretion (Koeth et al., 2013).

When [1,6-^{13}C] glucose and [1,2-^{13}C] acetate were infused together into mouse models, it was revealed through ^{13}C NMR that the tumor brain shows higher uptake of acetate than the normal brain (control) (Mashimo et al., 2014). Acetate metabolism is driven by FAO and the overexpression of Acetyl-CoA synthetase (ACSS2), which promotes acetate uptake, (Liu et al., 2022) impacts systemic levels and consequently its concentration in urine.

Glutamine performs a multitude of roles, ranging from replenishment of TCA cycle intermediates, nitrogen source for synthesis of amino acids, purines, and pyrimidines, as well as uptake of essential amino acids, activation of the mTOR (mammalian target of rapamycin) pathway, glutathione synthesis, and synthesis of glutamate in the brain (Mirveis et al., 2023; Newsholme et al., 2003). Despite being a non-essential amino acid, it becomes conditionally essential in glutamine addicted malignancies. (Obara-Michlewska & Szeliga, 2020; Wise et al., 2008). High glutamine flux due to increased expression of transporters (ASC2, LAT1) (Cormerais et al., 2018) accompanied by cancer-associated muscle proteolysis and hepatic amino-acid metabolism (Fearon et al., 2012) can influence its level in urine.

To cope with the persistent nutrient shortage, neoplasms need a supply of TCA cycle intermediates as the catabolic

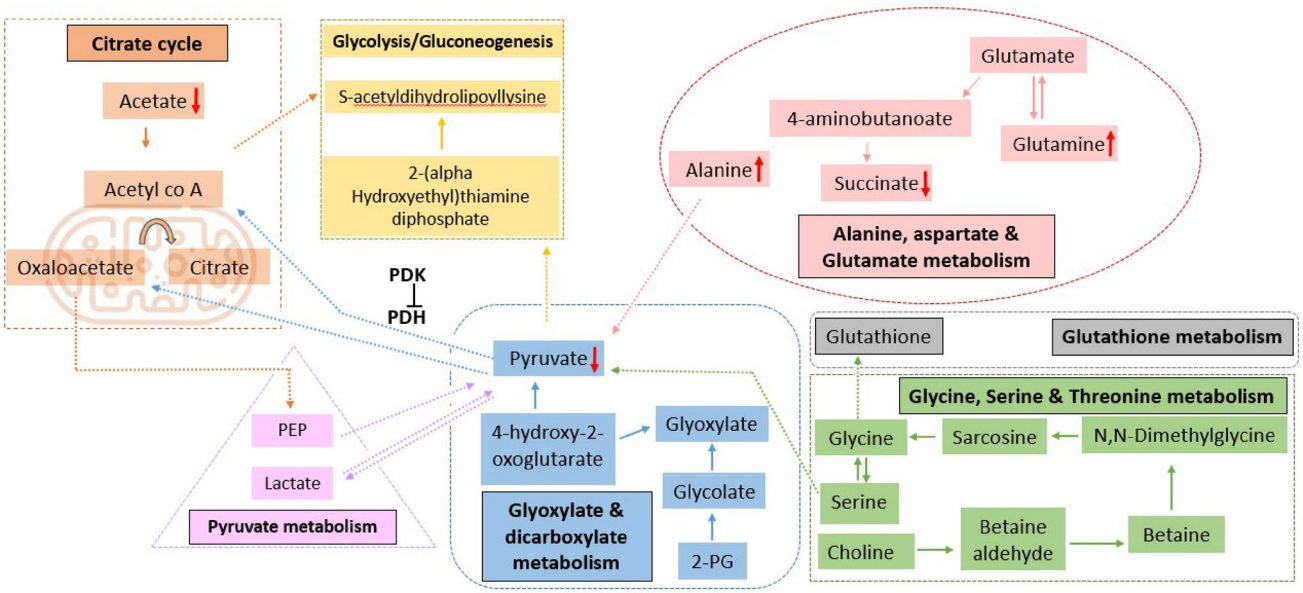

Fig. 9 Major pathways involved in the glioma metabolism as deduced from our analysis. Levels of the metabolites that were detected is shown with the help of red arrows. Direction of the arrows indicates their concentration in disease condition when compared with control

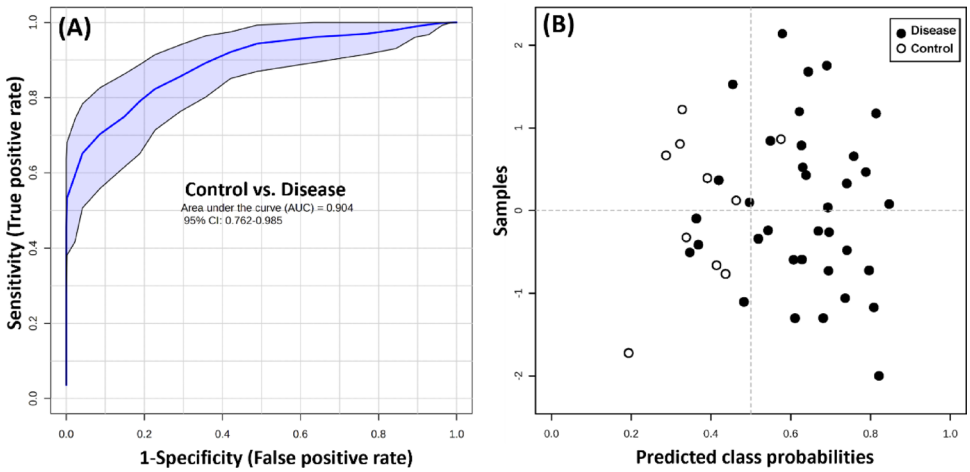

Fig. 10 **A** Multivariate ROC Curve constructed using the significant features shows the model's ability to predict whether the sample is of Control or Disease group, AUC for this curve was 0.90 with confidence interval from 0.76 to 0.98 indicating good diagnostic potential of the candidate metabolites as biomarker. **B** Predicted class probabilities for each sample given by the model

Table 5 Statistical data reveals the metabolites crucial for discrimination between Control vs. Disease and Control vs. individual grades. The listed metabolites came to be significant in fold change analysis (values are listed) where values > 1 in fold change shows that concentration was higher in urine of patients than in control. Cut off threshold for VIP score was taken to be 0.90, values were obtained from PLS-DA models. The statistically significant metabolites from *t*-test are marked with star

Comparison	Metabolites	VIP Score	Fold change	Level
Control vs. Disease	Alanine*	1.29	3.33	Up
	Succinate	0.94	3.20	Up
	Carnitine*	1.22	2.85	Up
	Lactate	0.91	2.33	Up
	2-hydroxybutyrate	1.67	2.12	Up
	Pyruvate*	1.49	0.49	Down
Control vs. Grade 2	Alanine	0.98	2.54	Up
	Carnitine	0.99	2.30	Up
	Adenine	1.04	2.08	Up
	2-hydroxybutyrate	1.48	2.01	Up
	Pyruvate	1.37	0.49	Down
	Succinate*	1.89	0.33	Down
	Propylene glycol	1.04	0.22	Down
Control vs. Grade 3	Alanine*	1.35	4.28	Up
	Carnitine*	1.39	2.96	Up
	Lactate	1.08	2.52	Up
	Acetate*	1.34	0.48	Down
	Trigonelline	1.15	0.46	Down
	Dimethylamine*	1.63	0.45	Down
	3-aminoisobutyrate	1.19	0.39	Down
	Pyruvate*	1.48	0.32	Down
Control vs. Grade 4	Alanine	1.23	3.42	Up
	Carnitine	1.22	3.24	Up
	2-Hydroxybutyrate	1.40	2.53	Up
	Adenine	0.90	2.08	Up

Table 6 1st Principal Component (PC1) and 2nd Principal Component (PC2) from Principal Component Analysis (PCA). R^2 and Q^2 values are from the cross-validation of the PLS-DA model. p-values are from permutation analysis of the model based on 1000 iterations

	PC1 (%)	PC2 (%)	R^2	Q^2	*p*-value
Control vs. Glioma	17.9	15.6	0.80	0.57	0.001
Control vs. different grades	17.9	15.6	0.80	0.51	0.01

processes are activated to promote biosynthesis. Pyruvate carboxylation and glutaminolysis are the two anaplerotic pathways that come to rescue under the above conditions, but the former is downregulated in malignant cells, and thus glutaminolysis, resulting in the formation of glutamate and ultimately α-ketoglutarate (a TCA cycle intermediate) becomes crucial for anaplerosis (DeBerardinis et al., 2007).

Disrupted energy metabolism is a hallmark of cancer cells. Pyruvate dehydrogenase (PDH) complex (PDC) is a multienzyme complex made of three components (E1, E2 and E3). The core of E1 PDH is composed of two α and two β subunits, and it decarboxylates pyruvate to form acetyl-CoA and therefore provides a link between glycolysis and the Krebs cycle. Pyruvate dehydrogenase kinase (PDK) inactivates PDH by phosphorylating serine residues in the α subunit of E1. PDK shows increased activity in glioma cells, thereby decreasing the rate of acetyl-CoA formation and increasing lactate production from pyruvate (Jha & Suk, 2013).

Apart from the perturbed energy balance that would result as a consequence of changes in succinate levels, succinate has also been implicated as an oncometabolite in tumorigenesis that can also bring about post-translational modifications in proteins (Zhang & Lang, 2023). Succinate was found to be altered significantly in grade 2 glioma as compared to the control.

Disturbed energy regulation, homeostasis, redox imbalance, and biosynthetic support are also evident from the pathways that are disturbed.

The urinary profile observed in our study is thus consistent with the profound metabolic rewiring observed in gliomas, supporting both enhanced glycolytic flux and reliance on other substrates. Changes in systemic amino acid

mobilization and cancer-specific catabolism, reflected by altered muscle proteolysis, are further evident from our findings. Together, these observations support increased substrate demand and the consequent host response, highlighting glioma-specific metabolic stress.

There is evidence that gliomas may cause partial disruption of the blood-brain barrier, resulting in systemic changes driven by the tumor (Digiovanni et al., 2024; Solar et al., 2022). It is thus essential to address and understand these metabolic alterations at a deeper level. This understanding can help establish non-invasive liquid biopsy biomarkers for timely diagnosis, monitoring treatment, and recurrence, and for the development of targeted metabolic therapies. Although this is a pilot study, the significant alterations observed in features such as glutamine, carnitine, and acetate, among others, may have potential as non-invasive markers for disease monitoring and treatment.

4.1 Future prospects

Novel targeted metabolic treatments can be explored, keeping in mind the alterations in metabolome. Inhibitors of different carnitine transporters responsible for increased carnitine flux can be employed to visualise the effect of reversing carnitine concentrations. The effect of blocking the PDK enzyme is another dimension that warrants further exploration. Pyruvate carboxylase-mediated anaplerotic flux is another central avenue that can be utilised to keep glioma cell proliferation under check.

Supplementary Information The online version contains supplementary material available at https://doi.org/10.1007/s11306-026-02414-8.

Acknowledgements The author would like to thank Indian Council of Medical Research for providing the fellowship grant (3/1/3/JRF-2021/HRD-009 1209744), Centre of Biomedical Research (CBMR) and Government of Uttar Pradesh for providing the lab facility and Academy of Scientific Innovation and Research (AcSIR) for the registration.

Author contributions AP: NMR experiment, data analysis and writing manuscript, AD: Sample and data collection, RV: analysis of data, AKJ: clinical data collection, data management, RK: provided control samples, KKD: Supervision, patient management and writing the manuscript, BB: Supervising the experimental NMR data and results and writing manuscript.

Funding The authors acknowledge DST-SUPREME for their funding (DST Project DST/SUPREME/2023/70) for our 800 MHz NMR spectrometer.

Data availability The raw data related to this article is available at Zenodo repository under the DOI https://doi.org/10.5281/zenodo.15378979.

Declarations

Conflict of interest The corresponding author states that there are no conflicts of interest on behalf of all the authors.

Ethical approval The study was ethically approved by the institutional ethics committee, SGPGIMS, Lucknow, India (2020-237-MCh-EXP-29, dated 08-09-2020).

Informed consent was obtained from all individuals in the study or from their first-degree relatives, and the participants have provided consent for the submission to the journal.

Open Access This article is licensed under a Creative Commons Attribution-NonCommercial-NoDerivatives 4.0 International License, which permits any non-commercial use, sharing, distribution and reproduction in any medium or format, as long as you give appropriate credit to the original author(s) and the source, provide a link to the Creative Commons licence, and indicate if you modified the licensed material. You do not have permission under this licence to share adapted material derived from this article or parts of it. The images or other third party material in this article are included in the article's Creative Commons licence, unless indicated otherwise in a credit line to the material. If material is not included in the article's Creative Commons licence and your intended use is not permitted by statutory regulation or exceeds the permitted use, you will need to obtain permission directly from the copyright holder. To view a copy of this licence, visit http://creativecommons.org/licenses/by-nc-nd/4.0/.

References

Amelio, I., Bertolo, R., Bove, P., Buonomo, O. C., Candi, E., Chiocchi, M., Cipriani, C., Di Daniele, N., Ganini, C., Juhl, H., Mauriello, A., Marani, C., Marshall, J., Montanaro, M., Palmieri, G., Piacentini, M., Sica, G., Tesauro, M., Rovella, V., … Melino, G. (2020). Liquid biopsies and cancer omics. *Cell Death Discovery*. https://doi.org/10.1038/S41420-020-00373-0

Araníbar, N., Ott, K. H., Roongta, V., & Mueller, L. (2006). Metabolomic analysis using optimized NMR and statistical methods. *Analytical Biochemistry*, *355*, 62–70. https://doi.org/10.1016/j.ab.2006.04.014

Armstrong, J. A. (2007). Urinalysis in western culture: A brief history. *Kidney International, 71*, 384–387. https://doi.org/10.1038/sj.ki.5002057

Baranovičová, E., Galanda, T., Galanda, M., Hatok, J., Kolarovszki, B., Richterová, R., & Račay, P. (2019). Metabolomic profiling of blood plasma in patients with primary brain tumours: Basal plasma metabolites correlated with tumour grade and plasma biomarker analysis predicts feasibility of the successful statistical discrimination from healthy subjects - A …. *IUBMB Life, 71*(12), 1994–2002. https://doi.org/10.1002/IUB.2149

Björkblom, B., Wibom, C., Jonsson, P., Mörén, L., Andersson, U., Johannesen, T. B., Langseth, H., Antti, H., & Melin, B. (2016). Metabolomic screening of pre-diagnostic serum samples identifies association between α- and ?-tocopherols and glioblastoma risk. *Oncotarget*, *7*, 37043–37053. https://doi.org/10.18632/oncotarget.9242

Bouatra, S., Aziat, F., Mandal, R., Guo, A. C., Wilson, M. R., Knox, C., Bjorndahl, T. C., Krishnamurthy, R., Saleem, F., Liu, P., Dame, Z. T., Poelzer, J., Huynh, J., Yallou, F. S., Psychogios, N., Dong, E., Bogumil, R., Roehring, C., & Wishart, D. S. (2013). The human urine metabolome. *PLoS ONE, 8*(9), Article e73076. https://doi.org/10.1371/JOURNAL.PONE.0073076

Brezmes, J., Llambrich, M., Cumeras, R., & Gumà, J. (2022). Urine NMR metabolomics for precision oncology in colorectal cancer. *International Journal of Molecular Sciences*. https://doi.org/10.3390/ijms231911171

Bruzzone, C., Loizaga-Iriarte, A., Loizaga-Iriarte, A., Sánchez-Mosquera, P., Gil-Redondo, R., Astobiza, I., Astobiza, I., Diercks, T., Cortazar, A. R., Cortazar, A. R., Ugalde-Olano, A., Ugalde-Olano, A., Schäfer, H., Blanco, F. J., Blanco, F. J., Unda, M., Unda, M., Cannet, C., Spraul, M., & Millet, O. (2020). ^{1}H NMR-based urine metabolomics reveals signs of enhanced carbon and nitrogen recycling in prostate cancer. *Journal of Proteome Research, 19*(6), 2419–2428. https://doi.org/10.1021/ACS.JPROTEOME.0C00091

Budczies, J., Denkert, C., Müller, B. M., Brockmöller, S. F., Klauschen, F., Györffy, B., Dietel, M., Richter-Ehrenstein, C., Marten, U., Salek, R. M., Griffin, J. L., Hilvo, M., Orešič, M., Wohlgemuth, G., & Fiehn, O. (2012). Remodeling of central metabolism in invasive breast cancer compared to normal breast tissue - a GC-TOFMS based metabolomics study. *BMC Genomics*. https://doi.org/10.1186/1471-2164-13-334

Carracedo, A., Cantley, L. C., & Pandolfi, P. P. (2013). Cancer metabolism: Fatty acid oxidation in the limelight. *Nature Reviews Cancer, 13*, 227–232. https://doi.org/10.1038/nrc3483

Chamberlain, M. C. (2010). Temozolomide: Therapeutic limitations in the treatment of adult high-grade gliomas. *Expert Review of Neurotherapeutics, 10*(10), 1537–1544. https://doi.org/10.1586/ERN.10.32

Chasapi, S. A., Karagkouni, E., Kalavrizioti, D., Vamvakas, S., Zompra, A., Takis, P. G., Goumenos, D. S., & Spyroulias, G. A. (2022). NMR-based metabolomics in differential diagnosis of chronic kidney disease (CKD) subtypes. *Metabolites, 12*(6), Article 490. https://doi.org/10.3390/METABO12060490/S1

Cheng, S. C., Chen, K., Chiu, C. Y., Lu, K. Y., Lu, H. Y., Chiang, M. H., Tsai, C. K., Lo, C. J., Cheng, M. L., Chang, T. C., & Lin, G. (2019). Metabolomic biomarkers in cervicovaginal fluid for detecting endometrial cancer through nuclear magnetic resonance spectroscopy. *Metabolomics*. https://doi.org/10.1007/s11306-019-1609-z

Console, L., Scalise, M., Mazza, T., Pochini, L., Galluccio, M., Giangregorio, N., Tonazzi, A., & Indiveri, C. (2020). Carnitine traffic in cells. Link with cancer. *Frontiers in Cell and Developmental Biology, 8*, Article 583850. https://doi.org/10.3389/FCELL.2020.583850/FULL

Cormerais, Y., Massard, P. A., Vucetic, M., Giuliano, S., Tambutté, E., Durivault, J., Vial, V., Endou, H., Wempe, M. F., Parks, S. K., & Pouyssegur, J. (2018). The glutamine transporter ASCT2 (SLC1A5) promotes tumor growth independently of the amino acid transporter LAT1 (SLC7A5). *Journal of Biological Chemistry, 293*(8), 2877. https://doi.org/10.1074/JBC.RA117.001342

DeBerardinis, R. J., Mancuso, A., Daikhin, E., Nissim, I., Yudkoff, M., Wehrli, S., & Thompson, C. B. (2007). Beyond aerobic glycolysis: Transformed cells can engage in glutamine metabolism that exceeds the requirement for protein and nucleotide synthesis. *Proceedings of the National Academy of Sciences of the United States of America, 104*, 19345–19350. https://doi.org/10.1073/pnas.0709747104

DeFeo, E. M., Wu, C. L., McDougal, W. S., & Cheng, L. L. (2011). A decade in prostate cancer: From NMR to metabolomics. *Nature Reviews Urology, 8*, 301–311. https://doi.org/10.1038/nrurol.2011.53

Diaz, P. M., Leehans, A., Ravishankar, P., & Daily, A. (2023). Multiomic approaches for cancer biomarker discovery in liquid biopsies: Advances and challenges. *Biomarker Insights*. https://doi.org/10.1177/11772719231204508

Digiovanni, S., Lorenzati, M., Bianciotto, O. T., Godel, M., Fontana, S., Akman, M., Costamagna, C., Couraud, P. O., Buffo, A., Kopecka, J., Riganti, C., & Salaroglio, I. C. (2024). Blood-brain barrier permeability increases with the differentiation of glioblastoma cells in vitro. *Fluids and Barriers of the CNS, 21*(1), Article 89. https://doi.org/10.1186/S12987-024-00590-0

Dinges, S. S., Hohm, A., Vandergrift, L. A., Nowak, J., Habbel, P., Kaltashov, I. A., Cheng, L. L., Nature Publishing Group. (2019). Cancer metabolomic markers in urine: Evidence, techniques and recommendations. *Nature Reviews Urology, 16*, 339–362. https://doi.org/10.1038/s41585-019-0185-3

Emwas, A. H., Roy, R., McKay, R. T., Ryan, D., Brennan, L., Tenori, L., Luchinat, C., Gao, X., Zeri, A. C., Gowda, G. A. N., Raftery, D., Steinbeck, C., Salek, R. M., & Wishart, D. S. (2016). Recommendations and standardization of biomarker quantification using NMR-based metabolomics with particular focus on urinary analysis. *Journal of Proteome Research, 15*, 360–373. https://doi.org/10.1021/acs.jproteome.5b00885

Fearon, K. C. H., Glass, D. J., & Guttridge, D. C. (2012). Cancer cachexia: Mediators, signaling, and metabolic pathways. *Cell Metabolism, 16*(2), 153–166. https://doi.org/10.1016/J.CMET.2012.06.011

Fink, M. A., Paland, H., Herzog, S., Grube, M., Vogelgesang, S., Weitmann, K., Bialke, A., Hoffmann, W., Rauch, B. H., Schroeder, H. W. S., & Bien-Moller, S. (2019). L-carnitine–mediated tumor cell protection and poor patient survival associated with OCTN2 overexpression in glioblastoma multiforme. *Clinical Cancer Research, 25*, 2874–2886. https://doi.org/10.1158/1078-0432.CCR-18-2380

Gao, H., Dong, B., Jia, J., Zhu, H., Diao, C., Yan, Z., Huang, Y., & Li, X. (2012). Application of ex vivo 1H NMR metabonomics to the characterization and possible detection of renal cell carcinoma metastases. *Journal of Cancer Research and Clinical Oncology, 138*, 753–761. https://doi.org/10.1007/s00432-011-1134-6

Hanif, F., Muzaffar, K., Perveen, K., Malhi, S. M., & Simjee, S. U. (2017). Glioblastoma multiforme: A review of its epidemiology and pathogenesis through clinical presentation and treatment. *Asian Pacific Journal of Cancer Prevention, 18*, 3–9. https://doi.org/10.22034/APJCP.2017.18.1.3

Horgan, R. P., & Kenny, L. C. (2011). 'Omic' technologies: Genomics, transcriptomics, proteomics and metabolomics. *The Obstetrician & Gynaecologist, 13*, 189–195. https://doi.org/10.1576/toag.13.3.189.27672

Jha, M. K., & Suk, K. (2013). Pyruvate dehydrogenase kinase as a potential therapeutic target for malignant gliomas. *Brain Tumor Research and Treatment, 1*, 57–63. https://doi.org/10.14791/btrt.2013.1.2.57

Jonsson, P., Antti, H., Späth, F., Melin, B., & Björkblom, B. (2020). Identification of pre-diagnostic metabolic patterns for glioma using subset analysis of matched repeated time points. *Cancers, 12*, 1–20. https://doi.org/10.3390/cancers12113349

Jothi, J., Janardhanam, V. A., & Krishnaswamy, R. (2020). Metabolic variations between low-grade and high-grade gliomas-profiling by 1H NMR spectroscopy. *Journal of Proteome Research, 19*(6), 2483–2490. https://doi.org/10.1021/ACS.JPROTEOME.0C00243

Juraszek, B., Czarnecka-Herok, J., & Nałęcz, K. A. (2021). Glioma cells survival depends both on fatty acid oxidation and on functional carnitine transport by SLC22A5. *Journal of Neurochemistry, 156*, 642–657. https://doi.org/10.1111/jnc.15124

Kelimu, A., Xie, R., Zhang, K., Zhuang, Z., Mamtimin, B., & Sheyhidin, I. (2016). Metabonomic signature analysis in plasma samples of glioma patients based on (1)H-nuclear magnetic resonance spectroscopy. *Neurology India, 64*(2), 246–251. https://doi.org/10.4103/0028-3886.177606

Koeth, R. A., Wang, Z., Levison, B. S., Buffa, J. A., Org, E., Sheehy, B. T., Britt, E. B., Fu, X., Wu, Y., Li, L., Smith, J. D., Didonato, J. A., Chen, J., Li, H., Wu, G. D., Lewis, J. D., Warrier, M., Brown,

J. M., Krauss, R. M., … Hazen, S. L. (2013). Intestinal microbiota metabolism of L-carnitine, a nutrient in red meat, promotes atherosclerosis. *Nature Medicine, 19*(5), 576–585. https://doi.org/10.1038/NM.3145

Larkin, J. R., Dickens, A. M., Claridge, T. D. W., Bristow, C., Andreou, K., Anthony, D. C., & Sibson, N. R. (2016). Early diagnosis of brain metastases using a biofluids- metabolomics approach in mice. *Theranostics, 6*, 2161–2169. https://doi.org/10.7150/thno.16538

Lee, J. E., Jeun, S. S., Kim, S. H., Yoo, C. Y., Baek, H. M., & Yang, S. H. (2019). Metabolic profiling of human gliomas assessed with NMR. *Journal of Clinical Neuroscience, 68*, 275–280. https://doi.org/10.1016/j.jocn.2019.07.078

Lin, H., Patel, S., Affeck, V. S., Wilson, I., Turnbull, D. M., Joshi, A. R., Maxwell, R., & Stoll, E. A. (2016). Fatty acid oxidation is required for the respiration and proliferation of malignant glioma cells. *Neuro-Oncology*, *19*(1), 43. https://doi.org/10.1093/NEUONC/NOW128

Liu, M., Liu, N., Wang, J., Fu, S., Wang, X., & Chen, D. (2022). Acetyl-CoA synthetase 2 as a therapeutic target in tumor metabolism. *Cancers, 14*(12), Article 2896. https://doi.org/10.3390/CANCERS14122896

Locasale, J. W. (2013). Serine, glycine and the one-carbon cycle: Cancer metabolism in full circle. *Nature Reviews. Cancer, 13*(8), Article 572. https://doi.org/10.1038/NRC3557

Louis, D. N., Perry, A., Wesseling, P., Brat, D. J., Cree, I. A., Figarella-Branger, D., Hawkins, C., Ng, H. K., Pfister, S. M., Reifenberger, G., Soffietti, R., Von Deimling, A., & Ellison, D. W. (2021). The 2021 WHO classification of tumors of the central nervous system: A summary. *Neuro-Oncology, 23*, 1231–1251. https://doi.org/10.1093/neuonc/noab106

Maher, E. A., Marin-Valencia, I., Bachoo, R. M., Mashimo, T., Raisanen, J., Hatanpaa, K. J., Jindal, A., Jeffrey, F. M., Choi, C., Madden, C., Mathews, D., Pascual, J. M., Mickey, B. E., Malloy, C. R., & Deberardinis, R. J. (2012). Metabolism of [U-13C] glucose in human brain tumors in vivo. *NMR in Biomedicine, 25*, 1234–1244. https://doi.org/10.1002/nbm.2794

Markley, J. L., Brüschweiler, R., Edison, A. S., Eghbalnia, H. R., Powers, R., Raftery, D., & Wishart, D. S. (2017). The future of NMR-based metabolomics. *Current Opinion in Biotechnology, 43*, 34–40. https://doi.org/10.1016/j.copbio.2016.08.001

Mashimo, T., Pichumani, K., Vemireddy, V., Hatanpaa, K. J., Singh, D. K., Sirasanagandla, S., Nannepaga, S., Piccirillo, S. G., Kovacs, Z., Foong, C., Huang, Z., Barnett, S., Mickey, B. E., Deberardinis, R. J., Tu, B. P., Maher, E. A., & Bachoo, R. M. (2014). Acetate is a bioenergetic substrate for human glioblastoma and brain metastases. *Cell, 159*(7), 1603–1614. https://doi.org/10.1016/j.cell.2014.11.025

Mirveis, Z., Howe, O., Cahill, P., Patil, N., & Byrne, H. J. (2023). Monitoring and modelling the glutamine metabolic pathway: A review and future perspectives. *Metabolomics*. https://doi.org/10.1007/s11306-023-02031-9

Mörén, L., Tommy Bergenheim, A., Ghasimi, S., Brännström, T., Johansson, M., & Antti, H. (2015). Metabolomic screening of tumor tissue and serum in glioma patients reveals diagnostic and prognostic information. *Metabolites, 5*(3), Article 502. https://doi.org/10.3390/METABO5030502

Mukherjee, A., Abraham, S., Singh, A., Balaji, S., & Mukunthan, K. S. (2024). From data to cure: A comprehensive exploration of multi-omics data analysis for targeted therapies. *Molecular Biotechnology, 67*(4), 1269–1289. https://doi.org/10.1007/S12033-024-01133-6

Neska-Matuszewska, M., Bladowska, J., Sąsiadek, M., & Zimny, A. (2018). Differentiation of glioblastoma multiforme, metastases and primary central nervous system lymphomas using multiparametric perfusion and diffusion MR imaging of a tumor core and a peritumoral zone—Searching for a practical approach. *PLoS ONE*. https://doi.org/10.1371/journal.pone.0191341

Newsholme, P., Lima, M. M. R., Procopio, J., Pithon-Curi, T. C., Doi, S. Q., Bazotte, R. B., & Curi, R. (2003). Glutamine and glutamate as vital metabolites. *Brazilian Journal of Medical and Biological Research, 36*, 153–163. https://doi.org/10.1590/S0100-879X2003000200002

Obara-Michlewska, M., & Szeliga, M. (2020). Targeting glutamine addiction in gliomas. *Cancers*. https://doi.org/10.3390/cancers12020310

Ohka, F., Natsume, A., & Wakabayashi, T. (2012). Current trends in targeted therapies for glioblastoma multiforme. *Neurology Research International, 2012*, Article 878425. https://doi.org/10.1155/2012/878425

Pang, Z., Lu, Y., Zhou, G., Hui, F., Xu, L., Viau, C., Spigelman, A. F., Macdonald, P. E., Wishart, D. S., Li, S., & Xia, J. (2024). MetaboAnalyst 6.0: Towards a unified platform for metabolomics data processing, analysis and interpretation. *Nucleic Acids Research, 52*, W398–W406. https://doi.org/10.1093/nar/gkae253

Ponti, A. K., Silver, D. J., Hine, C., & Lathia, J. D. (2024). Should i stay or should i go? Transsulfuration influences invasion and growth in glioblastoma. *Journal of Clinical Investigation, 134*(3), Article e176879. https://doi.org/10.1172/JCI176879

Ruiz-Rodado, V., Brender, J. R., Cherukuri, M. K., Gilbert, M. R., & Larion, M. (2021). Magnetic resonance spectroscopy for the study of cns malignancies. *Progress in Nuclear Magnetic Resonance Spectroscopy*, *122*, 23–41. https://doi.org/10.1016/j.pnmrs.2020.11.001

Shergalis, A., Bankhead, A., Luesakul, U., Muangsin, N., & Neamati, N. (2018). Current challenges and opportunities in treating glioblastomas. *Pharmacological Reviews*, *70*, 412–445. https://doi.org/10.1124/pr.117.014944

Shi, Y., Ding, D., Liu, L., Li, Z., Zuo, L., Zhou, L., Du, Q., Jing, Z., Zhang, X., & Sun, Z. (2021). Integrative analysis of metabolomic and transcriptomic data reveals metabolic alterations in glioma patients. *Journal of Proteome Research, 20*(5), 2206–2215. https://doi.org/10.1021/ACS.JPROTEOME.0C00697

Solar, P., Hendrych, M., Barak, M., Valekova, H., Hermanova, M., & Jancalek, R. (2022). Blood-brain barrier alterations and edema formation in different brain mass lesions. *Frontiers in Cellular Neuroscience, 16*, Article 922181. https://doi.org/10.3389/FNCEL.2022.922181

Sottoriva, A., Spiteri, I., Piccirillo, S. G. M., Touloumis, A., Collins, V. P., Marioni, J. C., Curtis, C., Watts, C., & Tavaré, S. (2013). Intratumor heterogeneity in human glioblastoma reflects cancer evolutionary dynamics. *Proceedings of the National Academy of Sciences of the United States of America, 110*, 4009–4014. https://doi.org/10.1073/pnas.1219747110

Stretch, C., Eastman, T., Mandal, R., Eisner, R., Wishart, D. S., Mourtzakis, M., Prado, C. M. M., Damaraju, S., Ball, R. O., Greiner, R., & Baracos, V. E. (2012). Prediction of skeletal muscle and fat mass in patients with advanced cancer using a metabolomic approach. *Journal of Nutrition*, *142*, 14–21. https://doi.org/10.3945/jn.111.147751

Tain, Y. L., & Hsu, C. N. (2017). Toxic dimethylarginines: Asymmetric Dimethylarginine (ADMA) and Symmetric Dimethylarginine (SDMA). *Toxins, 9*(3), Article 92. https://doi.org/10.3390/TOXINS9030092

Tandle, A. T., Shankavaram, U., Brown, M. V., Ho, J., Graves, C., Lita, E., Pfohl, J., Mohney, R., Tofilon, P., & Camphausen, K. (2013). Urinary Metabolomic Profiling of Patients with Glioblastoma Multiforme) Urinary Metabolomic Profiling of Patients with Glioblastoma Multiforme. *J Proteomics Bioinform*. https://doi.org/10.4172/jpb.S6-003

Tang, W. H. W., Wang, Z., Levison, B. S., Koeth, R. A., Britt, E. B., Fu, X., Wu, Y., & Hazen, S. L. (2013). Intestinal microbial

metabolism of phosphatidylcholine and cardiovascular risk. *New England Journal of Medicine, 368*(17), 1575–1584. https://doi.org/10.1056/NEJMOA1109400

Tynkkynen, T., Wang, Q., Ekholm, J., Anufrieva, O., Ohukainen, P., Vepsäläinen, J., Männikkö, M., Keinänen-Kiukaanniemi, S., Holmes, M. V., Goodwin, M., Ring, S., Chambers, J. C., Kooner, J., Järvelin, M. R., Kettunen, J., Hill, M., Davey Smith, G., & Ala-Korpela, M. (2019). Proof of concept for quantitative urine NMR metabolomics pipeline for large-scale epidemiology and genetics. *International Journal of Epidemiology, 48*(3), 978–993. https://doi.org/10.1093/IJE/DYY287

Virchow, R. (1863–1867). Die krankhaften Geschwülste dreissig Vorlesungen, gehalten während des Wintersemesters 1862–1863 an der Universität zu Berlin. (n.d.). In https://collections.nlm.nih.gov/catalog/nlm:nlmuid-62231840R-mvset

Wang, W., Ou, Z., Huang, X., Wang, J., Li, Q., Wen, M., & Zheng, L. (2024). Microbiota and glioma: A new perspective from association to clinical translation. *Gut Microbes, 16*(1), Article 2394166. https://doi.org/10.1080/19490976.2024.2394166

Weller, M., Wick, W., Aldape, K., Brada, M., Berger, M., Pfister, S. M., Nishikawa, R., Rosenthal, M., Wen, P. Y., Stupp, R., & Reifenberger, G. (2015). Glioma. *Nature Reviews Disease Primers, 1*(1), Article 15017-. https://doi.org/10.1038/nrdp.2015.17

Wise, D. R., Deberardinis, R. J., Mancuso, A., Sayed, N., Zhang, X. Y., Pfeiffer, H. K., Nissim, I., Daikhin, E., Yudkoff, M., McMahon, S. B., & Thompson, C. B. (2008). Myc regulates a transcriptional program that stimulates mitochondrial glutaminolysis and leads to glutamine addiction. *Proceedings of the National Academy of Sciences of the United States of America, 105*, 18782–18787. https://doi.org/10.1073/pnas.0810199105

Wyss, M., & Kaddurah-Daouk, R. (2000). Creatine and creatinine metabolism. *Physiological Reviews*, *80*(3), 1107–1213. https://doi.org/10.1152/PHYSREV.2000.80.3.1107

Yu, M. S., Chiu, C. Y., Lo, F. S., Lin, W. C., Wu, L. J., Yen, C. Y., & Yu, M. C. (2025). Dynamics of urine metabolomics and tubular inflammatory cytokines in type 1 diabetes across disease durations. *Metabolites, 15*(11), 734. https://doi.org/10.3390/METABO15110734/S1

Zhang, W., & Lang, R. (2023). Succinate metabolism: A promising therapeutic target for inflammation, ischemia/reperfusion injury and cancer. *Frontiers in Cell and Developmental Biology*. https://doi.org/10.3389/fcell.2023.1266973

Zhao, J., Ma, X., Gao, P., Han, X., Zhao, P., Xie, F., & Liu, M. (2024). Advancing glioblastoma treatment by targeting metabolism. *Neoplasia, 51*, Article 100985. https://doi.org/10.1016/J.NEO.2024.100985

Publisher's note Springer Nature remains neutral with regard to jurisdictional claims in published maps and institutional affiliations.